Diagn Interv Radiol 2024; DOI: 10.4274/dir.2025.253651

NEURORADIOLOGY

ORIGINAL ARTICLE



# Prognostic value of nidus sphericity in brain AVMs treated with Gamma Knife Radiosurgery: a preliminary study

Yunus Emre Şentürk[1]
Enes Muhammed Cantürk[1]
Ahmet Peker[1]
Sabahattin Yüzkan[1]
Selçuk Peker[2]

[1]Koç University Hospital, Department of Radiology, İstanbul, Türkiye

[2]Koç University Hospital, Department of Neurosurgery, İstanbul, Türkiye

**PURPOSE**

To evaluate the association of the three-dimensional (3D)-modelled sphericity index of brain arteriovenous malformation (AVM) with nidus obliteration rate and time following Gamma Knife® Radiosurgery (GKRS), and to compare the predictive value of the AVM nidus sphericity index with previously established morphological predictors, such as AVM volume.

**METHODS**

This institutional review board-approved retrospective study included 44 patients with cerebral AVMs who underwent single-session or hypofractionated GKRS between 2020 and 2023. Patients who received multimodal therapy, including prior endovascular embolization or microsurgical resection of the AVM nidus, were excluded. A minimum follow-up of 24 months was required for study inclusion. The primary endpoint was defined as complete angiographic obliteration following the initial GKRS, without any latent intracranial hemorrhage requiring hospitalization or surgical intervention. Pretreatment threshold-based semi-automatic segmentation of the AVM nidus was performed to obtain its volume and surface area, from which the sphericity index (Φ) was calculated.

**RESULTS**

Nineteen (43.2%) AVMs achieved obliteration at a mean of 35.7 ± 11.4 months, whereas 25 (56.8%) had residual nidus at 43.7 ± 13.4 months. Sphericity values were more compact and stable, whereas volume showed wide variability across the groups. The median volume of obliterated AVMs was 1.6 (3.9) $cm^3$, and the median volume for AVMs with residual nidus was 4.9(13.7) $cm^3$ ($P = 0.002$). Median AVM sphericity was 0.53 (0.26) for obliterated AVMs and 0.32 (0.19) for AVMs with residual nidus ($P = 0.003$). Sphericity demonstrated fair discriminative performance, comparable to AVM volume (Φ cut-off: 0.41; sensitivity 79%, specificity 68%, area under the curve: 0.77). However, optimal cut-off values of 0.30 and 0.66 yielded a sensitivity and specificity of 100% and 96%, respectively. Kaplan–Meier analysis revealed a shorter median obliteration time for high-sphericity AVMs (> 0.41) compared with low-sphericity AVMs (45 vs. 60 months, $P = 0.001$). Among patient-related and morphological parameters, sphericity was associated with earlier AVM obliteration (hazard ratio: 36.29, 95% confidence interval: 2.89–454.37, $P = 0.005$), although it did not remain an independent predictor in multivariate analysis.

**CONCLUSION**

This preliminary study found that higher AVM nidus sphericity was associated with increased obliteration rates and shorter time to obliteration following GKRS. Although not an independent predictor, sphericity exhibited a more stable distribution than volume, suggesting its potential as a complementary 3D biomarker for predicting radiosurgical outcomes of AVMs.

**CLINICAL SIGNIFICANCE**

AVM nidus sphericity may serve as a practical 3D geometric biomarker for predicting long-term outcomes following GKRS.

**KEYWORDS**

Arteriovenous malformation, Gamma Knife Radiosurgery, magnetic resonance imaging, Spetzler–Martin grade, sphericity

**Corresponding author:** Yunus Emre Şentürk

**E-mail:** ysenturk@kuh.ku.edu.tr

Received 15 September 2025; revision requested 24 October 2025; accepted 27 November 2025.

Epub: 13.01.2026

Publication date:

DOI: 10.4274/dir.2025.253651

You may cite this article as: Şentürk YE, Cantürk EM, Peker A, Yüzkan S, Peker S. Prognostic value of nidus sphericity in brain AVMs treated with Gamma Knife Radiosurgery: a preliminary study. *Diagn Interv Radiol.* XXX January 2026 DOI: 10.4274/dir.2025.253651 [Epub Ahead of Print].

Cerebral arteriovenous malformations (AVM) are rare complex vascular abnormalities with an annual incidence of 1.12 per 100,000 person-years.[1] The annual hemorrhage rate is 2.2% for unruptured AVMs and 3.0% for ruptured AVMs. The risk of hemorrhage is mostly associated with prior hemorrhage, deep location, presence of deep venous drainage, and associated aneurysms.[2] Cerebral AVM management remains under debate, especially for unruptured AVMs. Current strategies include observation, microsurgical resection, endovascular embolization, and stereotactic radiosurgery, or various combinations of these methods. Of these, the radiosurgical approach, particularly Gamma Knife® Radiosurgery (GKRS), is a well-recognized and effective approach for smaller and compact AVMs.[3,4] For larger AVMs [Spetzler–Martin (SM) grades 4 and 5], cerebral AVM treatment often requires a multimodal approach, including GKRS and neoadjuvant endovascular embolization to achieve AVM obliteration.[5] However, some reports have suggested that pre-GKRS neoadjuvant endovascular embolization may hinder accurate AVM delineation in high-grade AVMs during treatment planning and promote collateralization around the nidus, potentially reducing the likelihood of obliteration.[6] Although this remains controversial and neoadjuvant endovascular embolization is the more favored approach, GKRS alone may be considered for high-grade AVMs (SM grades 4 and 5) in some centers, typically requiring staged hypofractionated sessions to reduce nidus volume while preventing latent hemorrhage, which otherwise carries an annual bleeding risk of 2%–4% or more if untreated.[7] Nevertheless, achieving complete obliteration with standalone GKRS remains the primary endpoint for SM grade 4 and 5 AVMs, with reported rates ranging between 33% and 53%.[8]

Morphological determinants of cerebral AVM response to GKRS were comprehensively assessed in the largest pooled meta-analysis, which comprised 12 cohorts.[9] In addition to marginal dose, this study mostly examined the effect of AVM nidus size, volume, venous drainage pattern, anatomical location, and SM grade to GKRS response. The most impactful predictor of obliteration was a smaller AVM volume (< 10 $cm^3$), which consistently emerged as the strongest independent parameter associated with AVM obliteration following GKRS. Similarly, a lower SM grade correlated with higher obliteration rates; however, this effect was largely confounded by nidus size in multivariate modeling. Interestingly, the presence of deep venous drainage was associated with an increased probability of obliteration, although its contribution was far less pronounced than AVM volume. In contrast, deeper location and a history of prior embolization were identified as independent negative predictors, reducing the long-term AVM obliteration rate following GKRS.

Besides the classical morphological determinants for GKRS response of AVMs, the current segmentation techniques can allow measurement of three-dimensional (3D) features of AVMs and their potential impact on response status. In this context, a series study reported that a more compact AVM achieves better obliteration, and claimed that, in addition to nidus size, a well-defined AVM margin relative to brain parenchyma is another beneficial feature for achieving better radiosurgery response.[10] In addition to the compactness index—which quantifies the vascular proportion of the AVM nidus relative to the surrounding brain parenchyma—the sphericity index provides a numerical measure of a 3D structure, describing how closely the nidus approximates a perfect sphere and thereby reflecting the degree of AVM nidus dispersion. In contrast to the compactness of AVM, the sphericity of AVM measurement is a ratio of surface area to volume, which is most sensitive to AVM nidus elongation, lobulation, and surface irregularities that were mostly demonstrated in studies with solid tumors.[11,12] Regardless of the maximal diameter of AVMs, lower sphericity represents higher AVM surface area, thereby indicating more contact with surrounding brain parenchyma. This is an underexplored 3D parameter in the context of AVMs, with the first report demonstrating that low-nidal sphericity below 0.44 was strongly correlated with a high-risk of seizure incidence in AVMs.[13]

This preliminary study assesses the association between AVM nidus sphericity and the cerebral AVM obliteration in patients treated exclusively with single-session or hypofractionated GKRS, without adjunctive endovascular embolization or microsurgery. Furthermore, the study evaluates the predictive performance of sphericity and compares it with established parameters, such as AVM volume, in achieving obliteration following GKRS.

**Main points**

- Predicting long-term obliteration of brain arteriovenous malformations (AVMs) following Gamma Knife® Radiosurgery (GKRS) remains challenging.
- AVM nidus sphericity quantifies surface irregularity or elongations as a novel three-dimensional geometric biomarker.
- Higher nidus sphericity is associated with earlier and more frequent AVM obliteration following GKRS.

## Methods

### Study participants and neuroimaging follow-up

This single-center retrospective study was approved by the Clinical Ethical Committee of the Koç University Ethical Committee on Human Research (protocol number: 2025.386.IRB2.174, approval date: 11.09.2025). Given the retrospective design, informed consent was waived.

The inclusion criterion for this study comprised patients with AVMs who underwent GKRS at Koç University Hospital between January 2020 and December 2023. The following criteria determined exclusion: patients 1) aged < 3 years; 2) with active imaging surveillance of < 24 months following GKRS;[14] and 3) who had undergone prior neoadjuvant endovascular embolization or open surgical resection with residual cerebral AVM nidus. During the study period, a total of 168 patients with AVMs were treated with GKRS. Of these, 27 had undergone prior embolization, and 11 had prior surgical resection with residual nidus. Seventy-six cases did not meet the minimum 24-month follow-up requirement. After applying these exclusion criteria, 44 AVMs were eligible for final analysis. The patient selection flowchart is presented in Figure 1. The AVMs were graded according to the SM classification system.

All patients underwent annual imaging surveillance with time-of-flight (ToF) magnetic resonance angiography (MRA) and contrast-enhanced 3D T1-VIBE magnetic resonance imaging (CE-MRI). After 24 months, if no residual nidus was detected on MRA with CE-MRI, digital subtraction angiography (DSA) was performed to confirm AVM obliteration, defined as the absence of a visible nidus and early cerebral venous filling. If a residual nidus was detected beyond 24 months on MRA with CE-MRI, repeat GKRS was performed, and follow-up imaging was continued with MRA every 6 months until no residual nidus was observed. Final confirmation of AVM obliteration was then obtained via DSA. The primary endpoint was defined as complete AVM obliteration following GKRS without major delayed hemorrhage necessitating hospitalization or surgical in-

tervention. The need for a second single or hypofractionated GKRS during follow-up did not preclude meeting the primary endpoint, as, according to the series conducted by Chung et al.,[15] angiographic obliteration is often expected in an average of 66 months even after repeated GKRS sessions.

### Gamma Knife Radiosurgery procedure and dose planning

On the day of radiosurgery, stereotactic MRI and computed tomography (CT) were obtained without a frameless workflow. The stereotactic MRI protocol included isotropic 3D T2-SPACE (slice thickness: 1.5 mm; TR/TE: 2,500/321 ms; field of view: 230 × 230 mm; flip angle: 150°) and 3D post-contrast T1-VIBE (slice thickness: 1.5 mm; TR/TE: 11/4.7 ms; field of view: 230 × 230 mm; flip angle: 23°), both acquired on the same 1.5 T scanner. A 3D ToF-MRA sequence was also obtained (slice thickness: 1.5 mm; TR/TE: 25/7 ms; field of view: 230 × 230 mm; flip angle: 25°). In addition, a thin-slice stereotactic CT (slice thickness: 1.0 mm) was acquired with the head oriented parallel to the scanner table. The 3D post-contrast T1-VIBE, 3D T2-SPACE, and ToF-MRA datasets were rigidly fused in the GammaPlan planning system (Elekta AB, Stockholm, Sweden) for AVM nidus delineation. Stereotactic CT was used for distortion correction. When the AVM nidus was poorly visualized on both post-contrast T1-VIBE and ToF-MRA sequences, or when a dural/pial arteriovenous fistula or incomplete visualization of feeding arteries was suspected, additional two-dimensional (2D) biplanar DSA (posteroanterior and lateral projections) was performed to improve nidus delineation. In the present series, 2D biplanar DSA runs were co-registered in 11 (25%) cerebral AVM cases as an additional fourth element to the fused MRI stacks within the GammaPlan vascular module to improve AVM nidus delineation.

All patients were treated using the Leksell Gamma Knife® Icon™ (Elekta AB, Stockholm, Sweden) system. Mild sedation was administered, and a stereotactic frame was applied to achieve rigid head fixation. Treatment planning was performed individually using the GammaPlan module planning system with semiautomatic segmentation of the AVM nidus. Here, GKRS plans were generated to achieve the highest possible conformity to the segmented nidus while excluding feeding arteries. Isodose shaping was accomplished using multiple small isocenters to minimize dose to the perinidal brain parenchyma. The coverage index, defined as the percentage of nidus volume encompassed by the prescription (minimum) dose, was maintained at ≥ 95% for all targeted AVM volumes. The selectivity index was maintained above 0.75 for all AVM cases. The conformity index, representing the ratio between the prescription isodose volume and the AVM nidus volume, typically ranges between 1.0 and 1.5. A steep dose fall-off strategy (high-gradient index) was systematically preferred to avoid irradiation of adjacent eloquent parenchyma. Hence, the gradient index was maintained under 3 in all AVMs, and the marginal prescription isodose was set to the 50% isodose line. All single-fraction GKRS procedures were performed using the Leksell G frame.

Patients with an AVM < 3 cm and located in non-eloquent brain regions were typically treated with single-session GKRS, with marginal doses ranging from 15–25 Gy depending on nidus volume and proximity to critical structures. For larger AVMs (> 3 cm), or for cases with high-risk features (e.g., intranidal aneurysm, tortuous high-flow deep venous drainage, history of prior hemorrhage), or AVMs located in eloquent/critical regions (brainstem, optic tracts, corona radiata, perirolandic cortex, etc.), a hypofractionated GKRS scheme was used. This consisted of five consecutive daily fractions, each delivering 3–6 Gy, to reduce the risk of radiation-induced toxicity in adjacent white matter tracts and to minimize the chance of post-treatment hemorrhage. In the 5-day hypofractionated GKRS protocol, the frameless thermoplastic mask system was used to ensure reproducible positioning throughout all treatment fractions. Before each session, cone-beam CT verification was performed to confirm accurate head positioning and alignment with the treatment plan. An infrared laser marker was used to monitor any abnormal immobilization of the mask during the GKRS treatment.

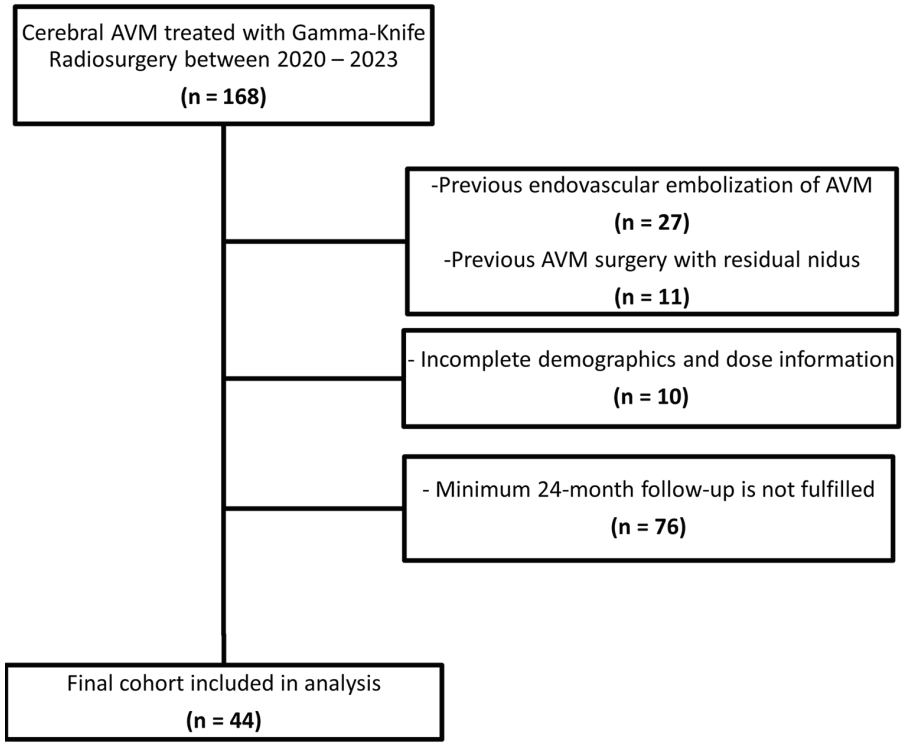


**Figure 1.** Summary flow chart of the study group selection process. AVM, arteriovenous malformation.

### Segmentation and image processing

All anonymized MRI data were analyzed by a neuroradiologist with 6 years of experience in the field of neuroimaging. The radiologist was blinded to all clinical information of the patients during the analysis. Three-dimensional volumetric T1-weighted gradient-echo images (3D T1-VIBE; voxel size: 1.0 × 1.0 × 1.0 mm) were imported into 3D Slicer (version 5.8.1; https://www.slicer.org) for image processing and sphericity analysis. Although both CE-3D T1-VIBE and ToF-MRA were performed, only the CE-T1-VIBE sequence was used as the reference dataset for AVM segmentation; ToF-MRA was not registered with the CE-T1-VIBE images, since flow-related signal attenuation and saturation effects in the former frequently lead to underestimation of the nidus size, particularly in regions of slow or turbulent flow. Flow-related signal attenuation in the AVM

nidus was more evident in the larger aneurysm (nidus size > 3cm) in ToF-MRA, which potentially biased the segmentation and led to a more artificially contracted nidus relative to an isotropic CE-T1-VIBE series.

The AVM nidus was initially delineated semiautomatically using a threshold-based segmentation approach on CE 3D T1-VIBE images. This process captured the enhancing nidus together with adjacent vascular structures, including feeding arteries, draining veins, and portions of normal vasculature. To refine the segmentation, the scissors tool in 3D Slicer was used to manually remove non-nidal vessels. An approximate 3-mm margin was preserved at the interface with feeding arteries to avoid inadvertent over-cutting of the nidus. The resulting volume was then rendered as a 3D surface. The segmentation method is illustrated in Figure 2. In contrast to prior radiomics studies of solid brain tumors, no Gaussian voxel-smoothing algorithm was applied since surface smoothing substantially inflates surface area measurements and artificially increases sphericity. Following completion of manual segmentation, the segment statistics module in 3D Slicer was used to compute the voxel-based volume and the surface mesh geometry of the AVM nidus. Given isotropic voxel dimensions of 1.0 $mm^3$, volume was calculated directly from voxel counts. Sphericity (Φ) was derived from volume (V) and surface area (A) using the following formula:

$$\Phi = \frac{\pi^{\frac{1}{3}} (6V)^{2/3}}{A}$$

### Statistical analysis

All statistical analyses were performed using IBM SPSS Statistics, version 28.0 (IBM Corp., Armonk, NY, USA). The analyses were primarily conducted by one of the authors (Y.E.S.), and all results were independently reviewed and verified by the co-authors, each of whom has substantial experience in medical statistics and data interpretation. Descriptive statistics were calculated for continuous variables, whereas categorical variables were summarized as frequencies and percentages. Normality of distribution for continuous variables was assessed using the Shapiro–Wilk test. The primary endpoint was defined as long-term GKRS outcome (> 24 months), dichotomized as complete obliteration vs. residual nidus. Group comparisons were performed according to the status of the primary endpoint. Normally distributed continuous variables were compared using the independent-samples t-test, whereas non-normally distributed variables were analyzed using the Mann–Whitney U test. Categorical variables were compared using Pearson's chi-square test. To assess segmentation reproducibility, one co-rater (A.P.) independently segmented the AVM nidus across the entire cohort. Inter-rater reliability for AVM volume and sphericity was evaluated using the intraclass correlation coefficient (ICC) derived from a two-way mixed-effects model. The diagnostic performance of AVM nidus sphericity and volume was evaluated using receiver operating characteristic (ROC) analysis, and optimal cut-off values were determined using the maximum Youden index in addition to maximum sensitivity and specificity strategies. Based on this threshold, AVMs were dichotomized into high-sphericity vs. low-sphericity groups. Kaplan–Meier survival analysis was then conducted to evaluate the association between sphericity status and time to obliteration following GKRS. Patients with residual AVM nidus who remained under imaging surveillance were censored at their last follow-up. Finally, univariate and multivariate Cox proportional hazards regression models were constructed to assess the relationship between time to obliteration and AVM morphologic parameters, age, and sex. A $P$ value < 0.05 was considered statistically significant in all analyses.

## Results

### Patient demographics and Gamma Knife Radiosurgery outcomes

A total of 44 patients (22 women/22 men) were deemed eligible for the study. The average follow-up time after the GKRS was 44.2 ± 15.7 months. Nineteen (43.2%) patients with AVM achieved the primary endpoint by displaying obliteration of the AVM nidus with a mean obliteration time of 35.7 ± 11.4 months. Out of 19 obliterated AVMs, 4 (13.8%) required a second GKRS with a mean marginal dose of 15.8 ± 1.5 Gy. Twenty-five (56.8%) patients with AVM did not achieve the primary endpoint and showed residual nidus despite marked volume reduction, with a mean last follow-up time after GKRS of 43.7 ± 13.4 months. Each of these cases required a second GKRS retreatment with a mean marginal dose of 20.2 ± 6.3 Gy. The patient demographics, GKRS parameters, and basic AVM features are listed in Table 1.

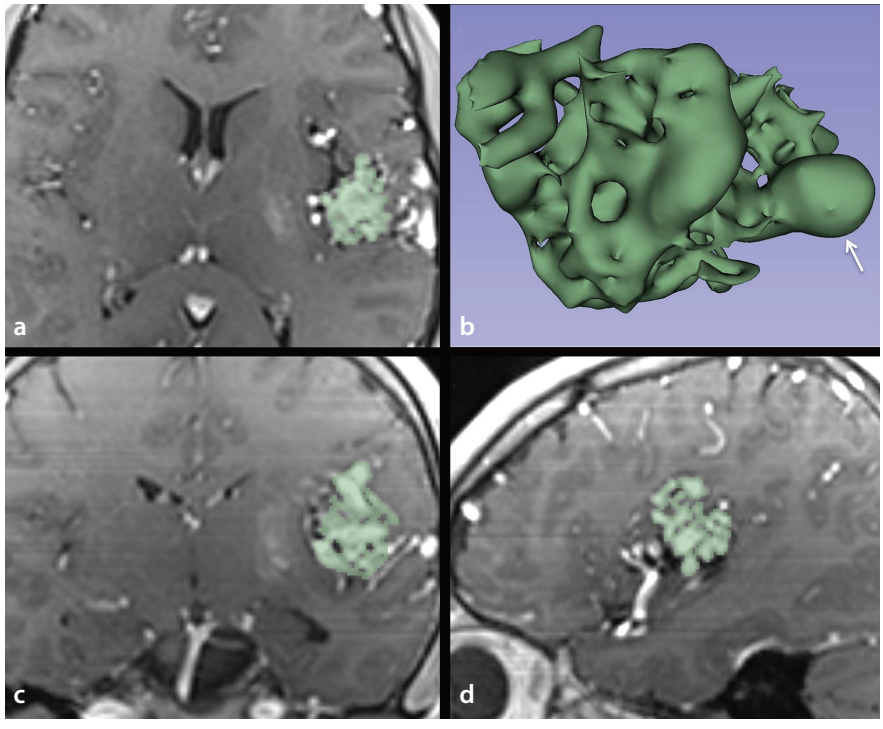


**Figure 2.** Illustration of brain arteriovenous malformation (AVM) segmentation. **(a, c, d)** Segmentation was performed on isotropic T1-weighted gradient-echo images (voxel size: 1.0 mm) for sphericity analysis. The AVM nidus was initially delineated semi-automatically using a threshold-based segmentation approach to distinguish the nidus from the surrounding brain parenchyma. Subsequently, the scissor tool was used to manually remove non-nidal vessels, such as feeding arteries beyond a 3-mm safety margin from the central nidus and large draining veins exiting the nidus. **(b)** Volume rendered three-dimensional view of segmented left insular AVM nidus. The Gaussian smoothing algorithm was exclusively avoided to prevent misrepresentation of the surface area. The measured AVM nidus surface area (A) was 21.16 $cm^2$, the nidus volume (V) was 2.68 $cm^3$, and the calculated sphericity index (Φ) was 0.44 for this patient. The arrow shows an intranidal aneurysm.

Among the 19 patients who achieved AVM obliteration, none experienced major intracranial hemorrhage requiring surgical intervention or hospitalization. One patient developed a minor localized hemorrhage at the site of the treated nidus following a single session of GKRS. In contrast, among the 25 patients with residual AVM nidus, 2 presented with self-limited subarachnoid hemorrhage within 1 year after GKRS, both requiring hospitalization without surgical or endovascular intervention.

### Sphericity and volume analysis of arteriovenous malformation in response to Gamma Knife Radiosurgery

Table 2 summarizes the distribution of patients, treatment characteristics, and AVM morphology according to GKRS response. Hypofractionated GKRS was 8.8-times more frequent in AVMs with residual nidus compared with those achieving obliteration ($P$ = 0.005). There was a trend toward significance in the marginal dose, with residual AVMs receiving a median of 25 (12) Gy vs. 20 (6) Gy in obliterated AVMs ($P$ = 0.060). Retreatment was required in four (13.8%) obliterated AVMs and in each of the residual AVMs, corresponding to a 7.3-fold-higher likelihood of retreatment in the residual group ($P$ = 0.001). The median AVM volume was 4.9 $cm^3$ in the residual group and 1.6 $cm^3$ in the obliterated group ($P$ = 0.002). Likewise, the median AVM sphericity was 0.53 in obliterated AVMs and 0.32 in those with residual nidus ($P$ = 0.001). Among patients achieving the primary endpoint, AVM size of 3–6 cm was the most frequent category (11 cases, 57.9%), whereas in the residual group, AVM size > 6 cm predominated (13 cases, 52%) ($P$ = 0.046). In line with this, the distribution of SM grade differed between groups, with SM grade 3 most common in obliterated AVMs and SM grade 4 most prevalent in residual AVMs ($P$ = 0.021).

**Table 1.** Patient demographics, AVM features, and GKRS outcomes

| Characteristic | Total (n = 44) |
|---|---|
| **Primary endpoint, n (%)** | |
| Obliteration | 19 (43.2%) |
| Residual nidus | 25 (56.8%) |
| **Age,** (mean ± SD) | 25.3 ± 13.4 |
| **Sex,** n (%) | |
| Male | 22 (50%) |
| Female | 22 (50%) |
| **Follow-up,** mo (mean ± SD) | 44.2 ± 15.7 |
| **Time to obliteration,** mo (mean ± SD) | 35.7 ± 11.4 |
| **Marginal dose,** (50 % isodose line), Gy, (mean ± SD) | 22.8 ± 7.1 |
| **Retreatment rate,** n (%) | 29 (65.9%) |
| **Latent bleeding following GKRS,** n (%) | 3 (6.8%) |
| **Location,** n (%) | |
| Lobar | 32 (72.8%) |
| Cerebellum | 4 (9.1%) |
| Thalamus | 3 (6.8%) |
| Corpus callosum | 2 (4.5%) |
| Basal ganglia | 1 (2.3%) |
| Brain stem | 2 (4.5%) |
| **Nidus size, cm** | |
| < 3cm | 20 (45.5%) |
| 3–6 cm | 17 (38.6%) |
| > 6 cm | 7 (15.9%) |
| **Intranidal aneurysm**, n (%) | 11 (25%) |
| **Deep venous drainage,** n (%) | 27 (61.4%) |
| **Spetzler–Martin grade,** n (%) | |
| 2 | 8 (18.2%) |
| 3 | 18 (40.9%) |
| 4 | 14 (31.8%) |
| 5 | 4 (9.1%) |
| **Clinical presentation,** n (%) | |
| Asymptomatic | 20 (45.5%) |
| Seizure | 15 (34.1%) |
| Bleeding | 4 (9.1%) |
| Sensorimotor symptoms | 4 (9.1%) |
| Visual symptoms | 1 (2.2%) |

AVM, arteriovenous malformation; GKRS, Gamma Knife Radiosurgery; SD, standard deviation

### Inter-rater reliability of segmented arteriovenous malformation volume and sphericity

The ICC was 0.94 [95% confidence interval (CI): 0.55–0.99] for AVM volume and 0.97 (95% CI: 0.86–0.99) for sphericity, indicating excellent inter-rater reliability in both parameters. However, the lower bound of the 95% CI for AVM volume was less than the ICC threshold of 0.70, commonly regarded as the cut-off for good agreement, suggesting that AVM volume measurements may be more susceptible to segmentation-related variability.

### Receiver operating characteristic curve analysis of arteriovenous malformation volume and sphericity for predicting long-term radiosurgical response

The ROC analysis results for AVM sphericity and volume are presented in Table 3. Here, AVM nidus sphericity demonstrated fairly good discriminative performance and a moderate positive correlation with long-term obliteration following GKRS (Spearman's ρ: 0.45, $P$ = 0.002). This finding indicates that as nidus sphericity increases, the likelihood of AVM obliteration following GKRS rises. The optimal sphericity cut-off of 0.41, derived from the best Youden index (0.469), yielded a sensitivity of 79%, specificity of 68%, and an area under the curve (AUC) of 0.77. The highest sensitivity (100%) was achieved at a cut-off of 0.30, whereas the highest specificity (96%) was achieved at a cut-off of 0.66. In contrast, AVM volume showed a moderate negative correlation with GKRS response (Spearman's ρ: –0.42, $P$ = 0.004). The distribution of AVM volume was highly variable, with extreme outliers particularly evident in large nidus sizes, ranging from 0.06 to 60.7

$cm^3$. This wide variability negatively impacted the robustness of volume-based cut-offs for predicting long-term GKRS outcomes. For the AVM nidus volume, the best cut-off value was 1.61 $cm^3$, which achieved a sensitivity of 53%, specificity of 92%, and AUC of 0.78, with the highest Youden index of 0.450. Maximum sensitivity (100%) was achieved at a 0.14-$cm^3$ cut-off, whereas maximum specificity (100%) was observed at a 15.6-$cm^3$ cut-off. Figure 3 illustrates a more stable and compact distribution of AVM nidus sphericity values compared with AVM volume, which demonstrated pronounced variability across the group.

### Effect of arteriovenous malformation morphologic features on obliteration time following Gamma Knife Radiosurgery

When patients were stratified by AVM sphericity according to the optimal cut-off (≤ 0.41: low sphericity, > 0.41: high sphericity), the median time to obliteration following GKRS was 45 months in the high-sphericity group and 60 months in the low-sphericity group ($P$ = 0.001), indicating a faster obliteration rate in AVMs with higher sphericity. Twenty-five patients with residual AVM nidus who did not reach the primary endpoint were censored in the survival analysis, as illustrated in Figure 4.

**Table 2.** Comparison of demographic data, AVM morphological features, and GKRS parameters based on treatment outcomes

| Variable | Obliterated AVM nidus (n = 19) | Residual AVM nidus (n = 25) | *P* value |
|---|---|---|---|
| **Age,** (mean ± SD) | 27.4 ± 15.8 | 23.7 ± 11.4 | 0.371 |
| **Sex** (F/M), | 10/9 | 12/13 | 0.763 |
| **Fractionation scheme (single/hypofractionated),** n | 15/4 | 11/14 | **0.005** |
| **Marginal dose,** median [IQR] | 20 [6] | 25 [12] | 0.060 |
| **Multiple-isocenter GKRS plan,** n (%) | 16 (84.2%) | 24 (96%) | 0.410 |
| **Number of isocenters per nidus,** median [IQR] | 9 [12] | 13 [8.0] | 0.204 |
| **Retreatment rate,** n (%) | 4 (13.8%) | 25 (100.0%) | **0.001** |
| **Retreatment dose,** median [IQR] | 15 [9] | 16 [10] | 0.090 |
| **AVM volume $cm^3$,** median [IQR] | 1.6 [3.9] | 4.9 [13.7] | **0.002** |
| **AVM surface area, $cm^2$** median [IQR] | 13.4 [26.3] | 44.2 [84.9] | **0.001** |
| **AVM sphericity, Φ,** median [IQR] | 0.53 [0.26] | 0.32 [0.19] | **0.003** |
| **Nidus size** | | | **0.046** |
| < 3cm | 1 (5.3%) | 6 (24%) | |
| 3–6 cm | 11 (57.9%) | 6 (24%) | |
| > 6cm | 7 (36.8%) | 13 (52%) | |
| **Intra-nidal aneurysm,** n (%) | 5 (26.3%) | 6 (24%) | 0.861 |
| **Deep venous drainage,** n (%) | 10 (52.6%) | 7 (28.0%) | 0.103 |
| **Spetzler–Martin grade,** n (%) | | | **0.021** |
| 2 | 6 (31.6%) | 2 (8%) | |
| 3 | 10 (52.6%) | 8 (32%) | |
| 4 | 2 (10.5%) | 12 (48%) | |
| 5 | 1 (5.3%) | 3 (12%) | |

AVM, arteriovenous malformation; GKRS, Gamma Knife Radiosurgery; IQR, interquartile range; SD, standard deviation; F, female; m, male

The impact of demographic and morphological factors on long-term AVM obliteration was first evaluated using a univariate Cox proportional hazards model. Variables that reached statistical significance were subsequently entered into a multivariate model to explore interdependence. The results are summarized in Table 4. Among the dose- and treatment-related variables, both the hypofractionation scheme and the use of multiple-isocenter treatment plans demonstrated only a trend toward a reduced hazard of earlier AVM obliteration without reaching statistical significance ($P$ = 0.060 for both). Among the morphological predictors, increased AVM sphericity had the highest positive hazard with faster obliteration [hazard ratio (HR): 36.29, 95% CI: 2.89–454.37, $P$ = 0.005], in contrast, larger AVM volume (HR: 0.88, 95% CI: 0.78–0.98, $P$ = 0.026) and higher SM grade (HR: 0.39, 95% CI: 0.21–0.71, $P$ = 0.002) were inversely associated with the early AVM obliteration, although their absolute hazard were notably smaller than that of sphericity. When these three morphological variables were analyzed together in the multivariate model, none retained independent predictive significance, suggesting that the predictive effect of sphericity is attenuated when adjusted for AVM volume and SM grade. Further variance inflation factor analysis yielded values of 2.82 for sphericity, 1.72 for volume, and 2.37 for SM grade, all below the conventional threshold for severe multicollinearity. Nevertheless, the limited sample size likely reduced the stability and independent predictive power of these parameters in the multivariate setting.

## Discussion

The present preliminary study highlights the prognostic value of the surface area-based sphericity index in predicting cerebral AVM obliteration following GKRS. In this preliminary cohort, higher sphericity was associated with both improved long-term AVM nidus obliteration outcomes and earlier achievement of obliteration following GKRS treatment. Unlike solid brain tumors

**Table 3.** Performance of AVM sphericity and volume in achieving the obliteration of AVM after the GKRS

| Variable | Cut-off | Youden index | AUC | Accuracy | Sensitivity,% | Specificity, % |
|---|---|---|---|---|---|---|
| **Sphericity** | 0.30 | 0.440 | 0.77 | 0.64 | 100 | 44 |
| **Sphericity** | **0.41** | **0.469*** | **0.77** | **0.73** | **79** | **68** |
| **Sphericity** | 0.66 | 0.223 | 0.77 | 0.64 | 26 | 96 |
| **Volume, $cm^3$** | 0.14 | 0.118 | 0.78 | 0.43 | 100 | 16 |
| **Volume, $cm^3$** | **1.61** | **0.450*** | **0.78** | **0.75** | **53** | **92** |
| **Volume, $cm^3$** | 15.6 | 0.280 | 0.78 | 0.57 | 28 | 100 |

*Highest Youden index value. AVM, arteriovenous malformation; GKRS, Gamma Knife Radiosurgery; AUC, area under the curve

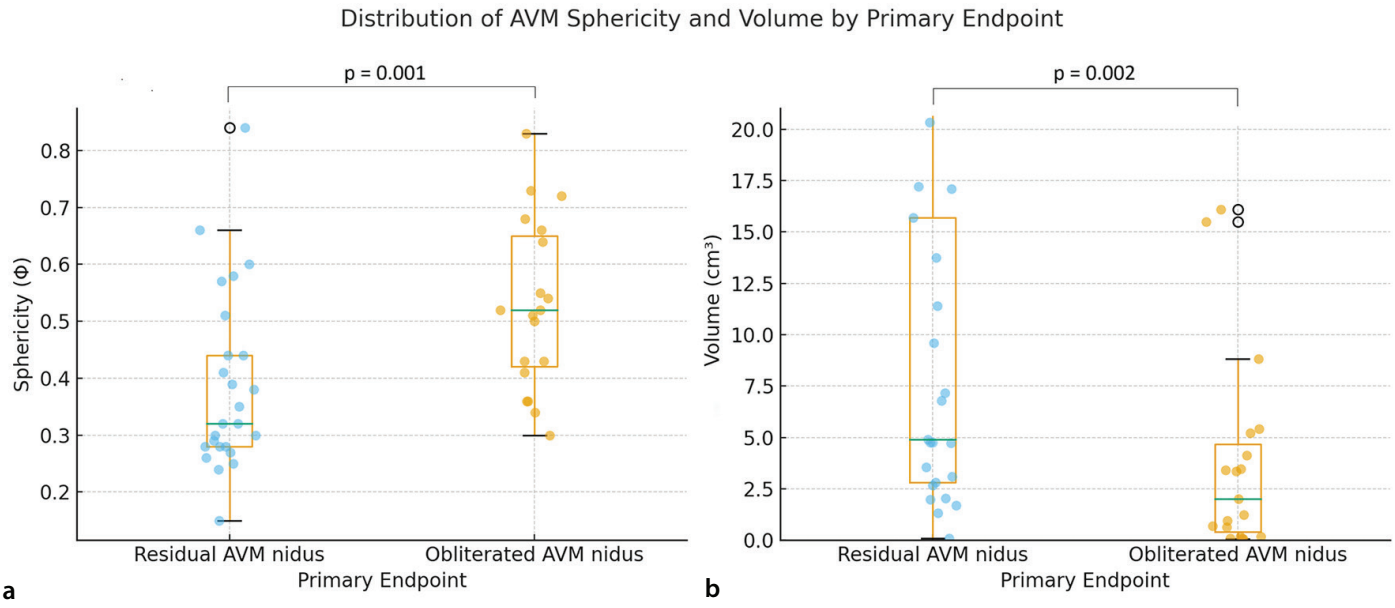


**Figure 3.** Boxplots showing the distribution of arteriovenous malformation (AVM) sphericity (Φ) and volume (V) according to treatment outcome, which is defined as residual vs. obliterated AVM nidus following Gamma Knife Radiosurgery. Sphericity index **(a)** showed a more compact and stable distribution compared with AVM volume **(b)**, which demonstrated wide variability and substantial overlap between groups.

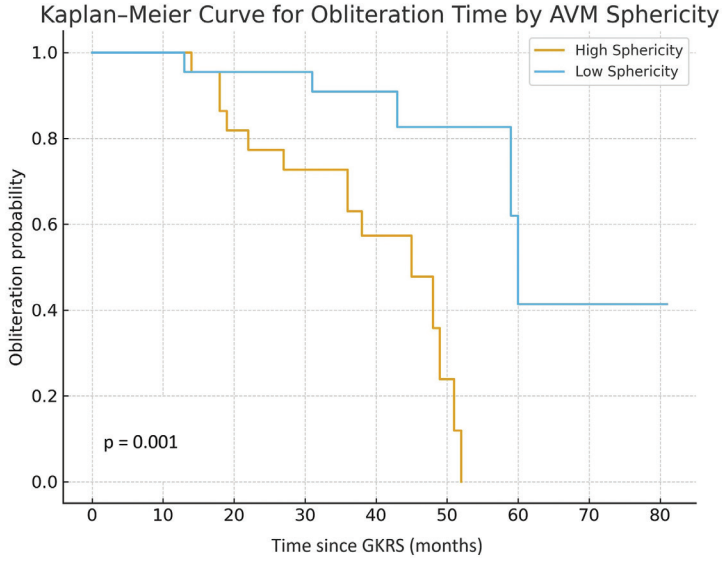


**Figure 4.** Kaplan–Meier analysis of arteriovenous malformation (AVM) obliteration time based on nidus sphericity. The AVMs were dichotomized according to the sphericity threshold of 0.41 (low sphericity: ≤ 0.41, high sphericity: > 0.41). Obliteration is defined as the primary endpoint. The median time to obliteration was 45 months for AVMs with a high-sphericity nidus and 60 months for AVMs with a low-sphericity nidus ($P$ = 0.001). GKRS; Gamma Knife® Radiosurgery.

or metastases, AVMs are inherently irregular and non-spherical structures; therefore, the sphericity values in the current study were lower than those typically reported in studies with solid tumors.[11,12] Nevertheless, obliterated AVMs demonstrated a median sphericity of 0.53 (0.26), compared with 0.32 (0.19) in AVMs with residual nidus. Using an optimal cut-off of 0.41, high-sphericity AVMs achieved obliteration at a median of 45 months, vs. 60 months in the low-sphericity group. These findings suggest that an AVM nidus with high sphericity correlates with shorter AVM obliteration time, whereas AVM volume and SM grade exert relatively smaller effects. However, sphericity did not retain independent predictive value in multivariate analysis for the AVM obliteration time, likely attributable to the limited sample size of the study.

Previous reports have consistently emphasized the nidus volume as the most robust structural feature for AVM obliteration.[9,16,17] Although our findings support this, the volume-based distribution of cerebral AVMs is extremely heterogeneous in the previous studies, leading to difficulties in determining the useful volume thresholds for achieving AVM obliteration. Marked differences in cerebral AVM volume make the pre-radiosurgical AVM volume clinically impractical to use as a prognostic parameter. Another caveat concerning AVM volume lies in the lack of knowledge on the extent of the nidal vascular distribution, such as a more compact AVM or dispersed AVM nidus may have a closer absolute AVM volume, although marginal radiation dose and time of obliteration, as well as the latent time to hemorrhage may differ from one another.[18] Therefore, the 3D features of AVM can be further elucidated to build a prognostic model for GKRS response. In the present cohort, the distribution of absolute nidal sphericity values effectively reflected the degree of surface irregularity within the nidus. The therapeutic principle of GKRS is based on endothelial injury and subsequent progressive fibrointimal hyperplasia leading to occlusion of the AVM nidus.[19] According to the radiomics-based tumor-shape study by Limkin et al.,[20] as sphericity decreases, intra-nidal irregularities and dispersion are expected to increase. Accounting for this consideration, a highly spherical AVM nidus can be expected to receive a more uniform radiation dose; however, when multiple isocenters and complex plugging techniques are applied, uniform dose distribution can be achievable across variable 3D nidus conformations. In our cohort, 40 (89.9%) AVMs were treated using a multiple-isocenter, complex plugging strategy, whereas only 4 cases were

**Table 4.** Cox proportional hazards model of AVM sphericity, morphological features, and demographics in relation to time to obliteration following GKRS

| | Univariate ( n = 44) | | Multivariate ( n = 44) | |
|---|---|---|---|---|
| Predictor | HR (95% CI) | *P* | HR (95% CI) | *P* |
| Age (year) | 1.02 (0.99–1.07) | 0.191 | | |
| Sex (female) | 0.91 (0.38–2.21) | 0.712 | | |
| Total marginal dose | 0.95 (0.88–1.03) | 0.213 | | |
| Fractionation scheme (hypofractionated) | 0.24 (0.06–1.04) | 0.060 | | |
| Multiple-isocenter GKRS plan | 0.29 (0.12–1.04) | 0.060 | | |
| Number of isocenters per nidus | 1.03 (0.96–1.10) | 0.394 | | |
| Spetzler–Martin grade | 0.39 (0.21–0.71) | **0.002** | 0.45 (0.160–1.29) | 0.142 |
| Intra-nidal aneurysm | 1.04 (0.36–2.99) | 0.936 | | |
| AVM volume ($cm^3$) | 0.88 (0.78–0.98) | **0.026** | 0.94 (0.82–1.08) | 0.383 |
| AVM sphericity | 36.29 (2.89–454.37) | **0.005** | 0.430 (0.01–59.74) | 0.734 |

AVM, arteriovenous malformation; HR, hazard ratio; GKRS, Gamma Knife Radiosurgery, CI, confidence interval

treated with a single, unplugged isocenter. The median number of isocenters did not differ significantly between the obliterated and residual AVM groups, suggesting that the use of multiple-isocenter planning is a consistent requirement across diverse nidus geometries to ensure therapeutic coverage. Therefore, the more favorable long-term obliteration outcomes observed in highly spherical AVMs may not be attributed only to distributed dose heterogeneity in the nidus but also to intrinsic anatomical factors, such as increased nidal vessel volume relative to surface area, which may enhance the effective bioavailability of therapeutic radiation even in complex AVM conformations.[21]

Earlier AVM obliteration has traditionally been associated with low nidus volume (< 10 $cm^3$) and lower SM grades. More recently, Pacini et al.[22] suggested that a high compactness index of the AVM nidus can be noted as a single independent quantitative predictor of AVM obliteration, demonstrating strong predictive capacity (AUC: 0.82; sensitivity: 97%; specificity: 52%). Our preliminary findings in this smaller cohort suggested that higher nidal sphericity is also associated with earlier AVM obliteration. However, the predictive performance of the sphericity index was not as robust as that of the compactness index in that series. Nonetheless, the direct comparison is not feasible as our cohort uniquely included AVMs treated exclusively with GKRS, whereas the Pacini et al. study comprised a larger group treated by multimodal strategies including endovascular embolization and open microsurgery.[22] Similar to the compactness index, our study demonstrated that a sphericity value > 0.41 may have predictive utility in achieving earlier AVM obliteration. Conceptually, compactness is defined as the vascular density within the parenchyma encompassing the AVM nidus,[23] whereas sphericity reflects surface irregularities and is presumed to be more sensitive to lobulations within an AVM nidus.[24] Notably, two AVM niduses with similar compactness values may differ substantially in terms of lobulation or sphericity. Therefore, integrating both compactness and sphericity indices as 3D parameters of AVM nidus, or developing automated software to calculate them, represents a promising research area that may offer new insights and facilitate early prediction of AVM obliteration following GKRS.

This study has several limitations, with the first being the retrospective single-center design and relatively small cohort size. The small cohort size may have reduced the statistical power for multivariate analysis, where the sphericity alone did not retain independent predictive capacity for AVM obliteration time. Nevertheless, the cohort was homogeneous, comprising only brain AVMs treated exclusively with GKRS. Second, AVM nidus segmentation was manually performed with semi-automated refinement, which is susceptible to inter-observer variability. Although the contouring was performed carefully and surface smoothing was avoided to preserve true geometric complexity, a certain extent of segmentation bias remains possible. Third, heterogeneity of treatment parameters, including marginal dose selection and use of hypofractionated vs. single-session GKRS, could have confounded AVM obliteration outcomes. Moreover, the compactness index was not specifically evaluated in this cohort, as the segmented 3D AVM nidus in the 3D Slicer environment did not precisely correspond to the planned treatment volume delineated by the prescription isodose boundaries within the radiosurgical treatment planning system. This discrepancy between anatomical and dosimetric segmentation volumes precluded reliable computation of the compactness index within the same workflow. Finally, although this study highlights the potential of sphericity as a novel geometric parameter, the absence of external validation of AVM nidus sphericity measurements represents another limitation, and the methodology should be further verified in larger independent cohorts. In the future, we plan to continue the analysis with a larger cohort.

In conclusion, the sphericity of the AVM nidus represents a measure of intra-nidal irregularity and elongation, and, therefore, the extent of nidal vascular surface area contacting the surrounding brain parenchyma. Although most AVM niduses do not approximate a true spherical shape, relatively higher sphericity values ($\Phi$ > 0.41) were moderately associated with improved radiosurgical response and higher obliteration rates. Compared with the absolute AVM nidus volume, the sphericity exhibited far more stable distribution, highlighting its potential role in refining prognostic models following GKRS. However, sphericity alone did not retain independent predictive value for AVM obliteration time, likely due to the limited sample size, which highlights the need for external validation. Despite these limitations, the present findings suggest that AVM nidus sphericity represents a practical and promising 3D geometric marker that warrants further validation in larger multicenter series to establish its predictive role for AVM obliteration.

## Footnotes

## Conflict of interest disclosure

The authors declared that there is no conflict of interest.

# References


1. Al-Shahi R, Bhattacharya JJ, Currie DG, et al. Prospective, population-based detection of intracranial vascular malformations in adults: the Scottish Intracranial Vascular Malformation Study (SIVMS). *Stroke*. 2003;34(5):1163-1169. [Crossref]
2. Gross BA, Du R. Natural history of cerebral arteriovenous malformations: a meta-analysis. *J Neurosurg*. 2013;118(2):437-443. [Crossref]
3. Kano H, Kondziolka D, Flickinger JC, et al. Stereotactic radiosurgery for arteriovenous malformations after embolization: a case-control study. *J Neurosurg.* 2012;117(2):265-275. [Crossref]
4. Yamamoto M, Jimbo M, Hara M, Saito I, Mori K. Gamma Knife Radiosurgery for arteriovenous malformations: long-term follow-up results focusing on complications occurring more than 5 years after irradiation. *Neurosurgery*. 1996;38(5):906-914. [Crossref]
5. Xiaochuan H, Yuhua J, Xianli L, Hongchao Y, Yang Z, Youxiang L. Targeted embolization reduces hemorrhage complications in partially embolized cerebral AVM combined with Gamma Knife Surgery. *Interv Neuroradiol*. 2015;21(1):80-87. [Crossref]
6. Kwon Y, Jeon SR, Kim JH, et al. Analysis of the causes of treatment failure in Gamma Knife Radiosurgery for intracranial arteriovenous malformations. *J Neurosurg*. 2000;93 Suppl 3:104-106. [Crossref]
7. Lauren C, Niryana IW, Mahadewa TGB. Impact of embolization on stereotactic radiosurgery outcomes for intracranial arteriovenous malformations Spetzler-Martin grades III-V: a systematic review and meta-analysis. *Front Surg*. 2025;12:1563256. [Crossref]
8. Byun J, Kwon DH, Lee DH, Park W, Park JC, Ahn JS. Radiosurgery for cerebral arteriovenous malformation (AVM): current treatment strategy and radiosurgical technique for large cerebral AVM. *J Korean Neurosurg Soc*. 2020;63(4):415-426. [Crossref]
9. Li W, Wang Y, Lu L, Zhang Y. The factors associated with obliteration following stereotactic radiosurgery in patients with brain arteriovenous malformations: a meta-analysis. *ANZ J Surg*. 2022;92(5):970-979. [Crossref]
10. Huang PW, Peng SJ, Pan DH, et al. Compactness index: a radiosurgery outcome predictor for patients with unruptured brain arteriovenous malformations. *J Neurosurg.* 2022;138(1):241-250. [Crossref]
11. Tarsitano A, Ricotta F, Cercenelli L, et al. Pretreatment tumor volume and tumor sphericity as prognostic factors in patients with oral cavity squamous cell carcinoma. *J Craniomaxillofac Surg*. 2019;47(3):510-515. [Crossref]
12. Ko PH, Kim HJ, Lee JS, Kim WC. Tumor volume and sphericity as predictors of local control after stereotactic radiosurgery for limited number (1-4) brain metastases from nonsmall cell lung cancer. *Asia Pac J Clin Oncol.* 2020;16(3):165-171. [Crossref]
13. Lin JY, Lu CF, Hu YS, et al. Magnetic resonance radiomics-derived sphericity correlates with seizure in brain arteriovenous malformations. *Eur Radiol*. 2024;34(1):588-599. [Crossref]
14. Graffeo CS, Sahgal A, De Salles A, et al. stereotactic radiosurgery for Spetzler-Martin grade I and II arteriovenous malformations: International Society of Stereotactic Radiosurgery (ISRS) Practice Guideline. *Neurosurgery*. 2020;87(3):442-452. [Crossref]
15. Chung Y, Park CK, Choi SK, Lim YJ. Long-term follow-up study of Gamma Knife Radiosurgery for arteriovenous malformations with diffuse-type nidi. *J Korean Soc Ster Func Neurosurg*. 2021;17(2):92-96. [Crossref]
16. Karlsson B, Lindquist C, Steiner L. Prediction of obliteration after Gamma Knife Surgery for cerebral arteriovenous malformations. *Neurosurgery*. 1997;40(3):425-430. [Crossref]
17. Kim MJ, Jung HH, Kim YB, et al. Comparison of single-session, neoadjuvant, and adjuvant embolization Gamma Knife Radiosurgery for arteriovenous malformation. *Neurosurgery*. 2023;92(5):986-997. [Crossref]
18. Huang PW, Peng SJ, Pan DH, et al. Vascular compactness of unruptured brain arteriovenous malformation predicts risk of hemorrhage after stereotactic radiosurgery. *Sci Rep.* 2024;14(1):4011. [Crossref]
19. Schneider BF, Eberhard DA, Steiner LE. Histopathology of arteriovenous malformations after gamma knife radiosurgery. *J Neurosurg*. 1997;87(3):352-357. [Crossref]
20. Limkin EJ, Reuzé S, Carré A, et al. The complexity of tumor shape, spiculatedness, correlates with tumor radiomic shape features. *Sci Rep.* 2019;9(1):4329. [Crossref]
21. Byun J, Kwon DH, Lee DH, Park W, Park JC, Ahn JS. Radiosurgery for cerebral arteriovenous malformation (AVM): current treatment strategy and radiosurgical technique for large cerebral AVM. *J Korean Neurosurg Soc*. 2020;63(4):415-426. [Crossref]
22. Pacini A, Shotar E, Granger B, et al. Niduscompacity determined by semi-automated segmentation is a strong quantitative predictor of brain arterio-venous malformation cure. *Clin Neuroradiol*. 2023;33(4):1095-1104. [Crossref]
23. Frisoli FA, Lang SS, Vossough A, et al. Intrarater and interrater reliability of the pediatric arteriovenous malformation compactness score in children. *J Neurosurg Pediatr*. 2013;11(5):547-551. [Crossref]
24. Cruz-Matías I, Ayala D, Hiller D, et al. Sphericity and roundness computation for particles using the extreme vertices model. *Journal of Computational Science*. 2019;30:28-40. [Crossref]